

Rigid Block Dynamics Confined between Side-Walls

S. J. Hogan

Phil. Trans. R. Soc. Lond. A 1994 **347**, 411-419

doi: 10.1098/rsta.1994.0051

Email alerting service

Receive free email alerts when new articles cite this article - sign up in the box at the top right-hand corner of the article or click [here](#)

To subscribe to *Phil. Trans. R. Soc. Lond. A* go to:
<http://rsta.royalsocietypublishing.org/subscriptions>

Rigid block dynamics confined between side-walls

BY S. J. HOGAN

*Department of Engineering Mathematics, University of Bristol, Queen's Building,
University Walk, Bristol BS8 1TR, U.K.*

A rigid block lies on a horizontal surface between two symmetrically placed walls. Under sinusoidal horizontal excitation, the block can impact both the floor and both side-walls. Periodic orbits are obtained analytically by linking piecewise linear solutions which have as an unknown the time impact difference between the floor and the wall. One nonlinear equation is then obtained in this unknown and solved numerically. The stability of these solutions is also examined. Symmetry-breaking and period-doubling bifurcations are observed. These latter responses can occur with larger than expected impact velocities. This problem has application in the nuclear industry where fuel rods can impact the sides of their containers. The design implication of these results is considered.

1. Introduction

The rocking of a free-standing rigid block under seismic excitation has been studied for over a century, particularly by workers in Japan. Early papers in the field include work by Milne (1881, 1885), Perry (1881), Milne & Omori (1893), Omori (1899, 1900) and Kirkpatrick (1927). This activity appears to have sprung from a suggestion of Mallett that earthquake magnitudes could be estimated in a quantitative way rather than through individual sensations, as had been the case. There was also the historical observation that many tall columns have survived known large earthquakes whereas other lower columns had collapsed. It was only later from the work of Housner (1963) that the diagonal length of a block (R in figure 1) was seen to play the crucial role in its dynamics, rather than its height H or its breadth B alone.

Practically speaking, the Japanese have long since exploited rocking block dynamics to estimate earthquake magnitudes. A traditional Japanese gravestone consists of a single engraved rectangular stone which stands freely on a stone plinth. When an earthquake strikes close enough to a graveyard, some of these headstones topple while others of different dimensions remain standing. A visit to a graveyard shortly after a tremor can provide useful estimates of the earthquake magnitude (Omote *et al.* 1977) using West's formula (Milne 1885); namely for the block to topple

$$a > gB/H, \quad (1.1)$$

where a is the magnitude of the horizontal component of acceleration due to the earthquake, and g is the acceleration due to gravity (see figure 1). Experiments by Milne & Omori (1893) suggest an empirical modification, introducing a factor of 0.935 to the right-hand side of equation (1.1). Housner's work could provide an even better estimate but West's formula has always been attractive because of its simplicity.

More recently, however, the nuclear industry safety regulators have demanded much more precise information about rocking block dynamics because many parts

Phil. Trans. R. Soc. Lond. A (1994) **347**, 411–419

© 1994 The Royal Society

Printed in Great Britain

411

17-2

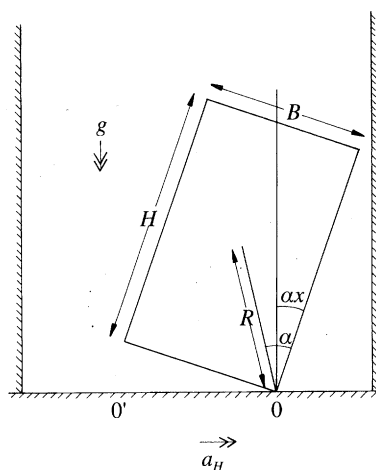


Figure 1. Sketch of rocking block with symmetrically placed side-walls.

of a nuclear installation involve free-standing items (e.g. computer equipment, fuel rods). Consequently the last ten years or so has seen an explosion of activity in this area with papers on block bouncing, sliding and rotating (Ishiyama 1982), two-storey structures (Psycharis 1990) and many more. There has also been interest in the subject from engineers working on conserving or rebuilding ancient monuments (see, for example, Oppenheim 1992). I was the first to apply the methods of dynamical systems to this problem (Hogan 1989), with some of the theoretical predictions being verified experimentally (Wong & Tso 1989; Hogan 1990). Since then the methods have been applied to problems involving damping due to external pipework (Hogan 1992*a*) and rocking confined to one corner (Hogan 1992*b*). In Hogan (1992*c*), heteroclinic bifurcations were found in the damped rigid block motion.

In this paper the simple undamped block is considered, rocking between the confining side-walls. This situation models that of fuel rods inside a reactor. An idealized configuration is sketched in figure 1, with the simplest problem of only one free rod being considered. During an earthquake the block may rock and impact on the side-walls, causing damage to the structure and possible fracture of the brittle rods. It is therefore of considerable interest to examine the dynamics of this problem and to understand the nature of the response of this system to an earthquake.

This paper is organized as follows. The equations governing the motion of the block are given in §2. In §3, a method is given to calculate asymptotic periodic responses of the block, and the stability of these solutions is examined in §4. The whole solution procedure is brought together in §5 and an illustrative example is given in §6. These results are discussed in §7.

2. Equations of motion

During the period of excitation the block will usually be considered to impact against one wall first, then the floor, then the opposite wall, and finally the floor again before restarting the cycle. Other motions involving different numbers of impacts on each wall may be possible, but one-sided rocking is excluded. We shall consider the existence and stability of periodic solutions to this system.

Taking moments about the point 0, we can write

$$I_0 \alpha x'' = -MgR \sin[\alpha(1-x)] - MRa \cos(\Omega\tau) \quad (2.1)$$

up to but not including impact with both wall and floor, where I_0 is the moment of inertia of the block about 0, M is the mass of the block, Ω is the frequency of excitation and τ is time. Prime indicates differentiation with respect to τ , and α , x and R are defined in figure 1. Similarly taking moments about $0'$, we find that, for a uniform block,

$$I_0 \alpha x'' = -MgR \sin[\alpha(1+x)] - MRa \cos(\Omega\tau). \quad (2.2)$$

It is well known that

$$I_0 = \frac{4}{3}MR^2 \quad (2.3)$$

and we can define

$$p^2 = MgR/I_0 = \frac{3}{4}g/R. \quad (2.4)$$

We then write non-dimensional time as $t = p\tau$, non-dimensional frequency $\omega = \Omega/p$, and non-dimensional amplitude $\beta = a/(\alpha g)$. In the limit of a slender block, (2.1) and (2.2) become

$$\ddot{x} - x + 1 = -\beta \cos(\omega t), \quad 0 < x < d, \quad (2.5)$$

$$\ddot{x} - x - 1 = -\beta \cos(\omega t), \quad -d < x < 0, \quad (2.6)$$

where the impact points are located symmetrically either side of the block but the walls themselves do not necessarily have to be either vertical or planar, d is the scaled angular position of the point of impact with the wall, and the horizontal distance between the point of impact with the wall and the nearest corner is given by $H \sin \alpha d$.

During the time the block is rotating about one corner or other, its motion is actually further subdivided into two (usually unequal) parts. For $0 < x < d$, let x_1 denote motion before impact with the wall and x_2 motion after impact. Thus x_1 and x_2 separately satisfy (2.5) and

$$\left. \begin{aligned} x_1(t_0) = 0, \quad x_1(t_1) = d, \quad x_2(t_1) = d, \quad x_2(t_2) = 0, \\ \dot{x}_2(t_1) = -q\dot{x}_1(t_1), \end{aligned} \right\} \quad (2.7)$$

where t_0 = time of one impact with the ground, t_1 = time of impact with the wall, t_2 = time of next impact with the ground and q = coefficient of restitution between block and wall.

For a rocking motion that is the same about $0'$ as it is about 0, then we have two further conditions to supplement (2.5)–(2.7) namely

$$\dot{x}_1(t_0) = -r\dot{x}_2(t_2), \quad (2.8)$$

$$t_2 - t_0 = n\pi/\omega, \quad (2.9)$$

where r is the coefficient of restitution between the block and the floor, and n is the number of drive periods in the periodic response. It is straightforward to show that n must be odd in this case. The motion governed by (2.5)–(2.9) is sketched in figure 2 in the phase plane (x, y) where $y = \dot{x}$. Note that we specifically exclude the non-physical case $q = r = 1$ from our analysis. The next stage is to find those parameter values for which periodic responses exist and then to ascertain whether or not such orbits are stable.

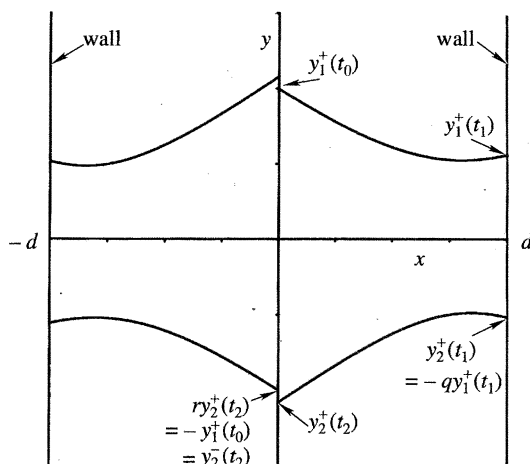


Figure 2. Sketch of typical response in phase plane, together with various definitions of quantities referred to in text.

3. Periodic responses

For symmetric responses it is sufficient to consider only the case $x > 0$. Hence from (2.1),

$$x_1(t) = A_1 \sinh(t - t_0) + A_2 \cosh(t - t_0) + \gamma \cos(\omega t) + 1, \quad (3.1)$$

$$x_2(t) = A_3 \sinh(t - t_1) + A_4 \cosh(t - t_1) + \gamma \cos(\omega t) + 1, \quad (3.2)$$

where the coefficients A_i ($i = 1-4$) depend on t_1, t_0 and the system parameters, but not on t . Equations (2.7) and (2.8) and the definition of t_2 , equation (2.9), are now used to find these coefficients and the quantity $(t_1 - t_0)$.

In fact,

$$A_1 = [d - 1 - \gamma \cos(\omega t_1) + \cosh(t_1 - t_0) [1 + \gamma \cos(\omega t_0)]] / \sinh(t_1 - t_0), \quad (3.3)$$

$$A_2 = -1 - \gamma \cos(\omega t_0), \quad (3.4)$$

$$A_3 = [-1 + \gamma \cos(\omega t_0) + \cosh(t_2 - t_1) [1 - d + \gamma \cos(\omega t_1)]] / \sinh(t_2 - t_1), \quad (3.5)$$

$$A_4 = d - 1 - \gamma \cos(\omega t_1), \quad (3.6)$$

where
$$\gamma = \beta / (1 + \omega^2). \quad (3.7)$$

After considerable manipulation it can be shown that

$$c_0 = \cos(\omega t_0) = (\mathcal{C}T - \mathcal{A}Y) / (\mathcal{C}\mathcal{B} - \mathcal{A}\mathcal{D}) \quad (3.8)$$

and

$$s_0 = \sin(\omega t_0) = (\mathcal{B}Y - \mathcal{D}T) / (\mathcal{C}\mathcal{B} - \mathcal{A}\mathcal{D}), \quad (3.9)$$

where

$$\mathcal{A} = P - Rc_{10} + Ss_{10}, \quad \mathcal{B} = Q - Rs_{10} - Sc_{10},$$

and

$$\mathcal{C} = U - Wc_{10} + Xs_{10}, \quad \mathcal{D} = V - Ws_{10} - Xc_{10},$$

$$P = B, \quad Q = \gamma D, \quad R = -C, \quad S = \gamma A, \quad T = A(1 - d) - D, \quad U = H, \quad V = \gamma(E - F),$$

with

$$W = -G, \quad X = -\gamma I, \quad Y = I(d - 1) + E + F,$$

$$\begin{aligned} A &= 1 - rqch_{21}ch_{10} + rsh_{21}sh_{10}, & B &= -\gamma\omega(1 - r)sh_{10}, & C &= \gamma\omega(1 + q)rch_{21}sh_{10}, \\ D &= -rqch_{21} + ch_{10}, & E &= 1 - rqch_{21}ch_{10}, & F &= qsh_{21}sh_{10}, & G &= -\gamma\omega(1 + q)sh_{21}, \\ H &= \gamma\omega(1 - r)qch_{10}sh_{21}, & I &= ch_{21} - rqch_{10} \end{aligned}$$

and
where

$$\begin{aligned}sh_{21} &= shch_{10} - chsh_{10}, & ch_{21} &= chch_{10} - shsh_{10}, \\s_{10} &= \sin[\omega(t_1 - t_0)], & c_{10} &= \cos[\omega(t_1 - t_0)], \\sh_{10} &= \sinh(t_1 - t_0), & ch_{10} &= \cosh(t_1 - t_0), \\sh &= \sinh(n\pi/\omega), & ch &= \cosh(n\pi/\omega).\end{aligned}$$

Equations (3.8) and (3.9) naturally lead to the implicit equation for $(t_1 - t_0)$

$$(\mathcal{C}T - \mathcal{A}Y)^2 + (\mathcal{B}Y - \mathcal{D}T)^2 = (\mathcal{C}\mathcal{B} - \mathcal{A}\mathcal{D})^2. \quad (3.10)$$

It is possible to simplify (3.10) further but no real advantage seems to stem from such a step, and a numerical solution appears inevitable.

To solve equation (3.10) it is only necessary to know the system parameters r , q and d , the forcing parameters β and ω and the period n of the response. Once $(t_1 - t_0)$ is found, it is straightforward to find $(t_2 - t_1)$ from equation (2.9). The time t_0 can be found from either (3.8) or (3.9), and hence both t_1 and t_2 follow. The constants A_i ($i = 1-4$) can then be calculated and the solutions $x_1(t)$, $x_2(t)$ are easily obtained. Note that (3.10) does not produce a unique solution for $(t_1 - t_0)$. However, it is a straightforward matter to discard all but one of the solutions on physical grounds. It is possible to extend this method to include periodic responses in which the ground and walls are impacted against more than once in each half-cycle, but the analysis becomes increasingly complicated and will not be pursued here.

4. Stability considerations

Not all of the asymptotic responses that can be found by the method of the previous section will be stable. It is therefore necessary to examine what happens to a perturbation as the response progresses. As before, such an analysis is best carried out in the phase plane.

Suppose that at time t_0 the block is at $x = 0^+$ with positive velocity $y_1^+(t_0)$ (see figure 2). At time t_1 , it impacts the wall at $x = d$ with velocity $y_1^+(t_1)$ and rebounds with velocity $y_2^+(t_1) = -ry_1^+(t_1)$. Subsequently it impacts the floor $x = 0^+$ at time t_2 with velocity $y_2^+(t_2)$ and commences the next part of its motion with velocity $y_2^+(t_2) = ry_2^+(t_2) = -y_1^+(t_0)$ by symmetry. We consider the fate of a small perturbation $\delta\mathbf{v}(t_0) = (\delta t_0, \delta y_1(t_0))^T$ as the motion proceeds. Symbolically

$$\delta\mathbf{v}(t_2) = N \cdot \delta\mathbf{v}(t_0) \quad (4.1)$$

where the matrix N is given in the Appendix.

The stability condition is clear from (4.1), namely that we must have $|\lambda_i| < 1$ ($i = 1, 2$) where the λ_i are eigenvalues of the matrix N . Instability will occur whenever one of these eigenvalues crosses the unit circle. Hence finding those parameter values for which $|\lambda_i| = 1$ corresponds to finding the boundary between stable and unstable solutions. In fact it can be shown that for this problem

$$\det N = q^2 r^2 \quad (4.2)$$

which is strictly less than 1 for parameter values used in this analysis. Hence, using the general result

$$\det N = \lambda_1 \lambda_2, \quad (4.3)$$

it can be seen that the only way the eigenvalues can cross the unit circle is along the real axis, that is, when $\lambda = \pm 1$. Consequently there are no Hopf bifurcations.

As

$$\lambda_{1,2} = \frac{1}{2}(\text{tr } N \pm [(\text{tr } N)^2 - 4 \det N]^{\frac{1}{2}}), \quad (4.4)$$

the problem of finding the stability boundaries $\lambda = \pm 1$ reduces to finding solutions of the equation

$$1 + \det N \mp \text{tr } N = 0. \quad (4.5)$$

The trace of the matrix N is given by

$$\begin{aligned} \text{tr } N = \frac{-q^2 r}{[A_1 - \gamma \omega s_0][A_3 - \gamma \omega s_1]} & \left\{ \left[(\mathcal{P} s h_{10} - \mathcal{R} c h_{10})(\mathcal{T} s h_{21} - \mathcal{V} c h_{21}) \right. \right. \\ & \left. \left. - \frac{s h_{10}}{q} (\mathcal{U} \mathcal{V} - \mathcal{W} \mathcal{T}) \right] (-r) + s h_{21} (2\mathcal{R} - \mathcal{P} \mathcal{S}) - \frac{\mathcal{S} \mathcal{W}}{q} \right\}, \quad (4.6) \end{aligned}$$

where

$$\begin{aligned} \mathcal{P} &= \gamma \omega^2 c_1 + (1 + \gamma c_0) c h_{10} - A_1 s h_{10}, \\ \mathcal{Q} &= \gamma \omega^2 c_0 c h_{10} + \gamma \omega s_0 s h_{10} + (1 + \gamma c_0) c h_{10} - A_1 s h_{10}, \\ \mathcal{R} &= \gamma \omega s_1 + (1 + \gamma c_0) s h_{10} - A_1 c h_{10}, \\ \mathcal{S} &= \gamma \omega^2 c_0 s h_{10} + \gamma \omega s_0 c h_{10} + (1 + \gamma c_0) s h_{10} - A_1 c h_{10}, \\ \mathcal{T} &= \gamma \omega^2 c_2 + (1 - d + \gamma c_1) c h_{21} - A_3 s h_{21}, \\ \mathcal{U} &= \gamma \omega^2 c_1 c h_{21} + \gamma \omega s_1 s h_{21} + (1 - d + \gamma c_1) c h_{21} - A_3 s h_{21}, \\ \mathcal{V} &= \gamma \omega s_2 + (1 - d + \gamma c_1) s h_{21} - A_3 c h_{21}, \\ \mathcal{W} &= \gamma \omega^2 c_1 s h_{21} + \gamma \omega s_1 c h_{21} + (1 - d + \gamma c_1) s h_{21} - A_3 c h_{21}, \end{aligned}$$

and

$$s_1 = \sin(\omega t_1), \quad c_1 = \cos(\omega t_1).$$

5. Solution procedure

Given the values of r , q and d as well as β , ω and n we are now able to see if an asymptotic periodic solution exists at these parameter values and then to examine its stability. The first part of this procedure was discussed in §3 where the times of impact t_0 and t_1 (as well as t_2) were calculated. The second part is straightforward to implement in that the same information is used to calculate $\det N$ from (4.2) and $\text{tr } N$ from (4.6). In this way $\lambda_{1,2}$ can easily be found from (4.4). Provided $|\lambda_i| < 1$ for $i = 1, 2$ the chosen solution will be stable. Then a particular parameter, say β , is varied and the whole procedure repeated. If $|\lambda_1|$ or $|\lambda_2|$ ever exceeds 1, a bifurcation has occurred and the solution is unstable. In practice, however, this whole procedure is cumbersome and it is more sensible to find the zero of equation (4.5). In principle then it is possible to calculate the stability boundaries by systematic variation of parameters. Finally we can obtain plots of the stable phase plane solutions by simple numerical integration of equations (2.1) and (2.2), adopting a similar technique to that of Hogan (1989).

6. Illustrative example

For $\omega = 1$, $d = 1$, $r = q = 0.925$, $n = 1$ and $\beta = 0.6$, the analysis of §3 reveals that $t_0 = 1.70848$, $t_1 = 3.25213$ and $t_2 = 4.85007$ with $y_1^+(t_0) = 0.8868$, $y_1^+(t_1) = 0.7889$.

The orbit is stable. Direct numerical integration, on the other hand, reveals that $t_0 = 1.70854$, $t_1 = 3.25212$ and $t_2 = 4.85014$ and $y_1^+(t_0) = 0.8868$, $y_1^+(t_1) = 0.7889$.

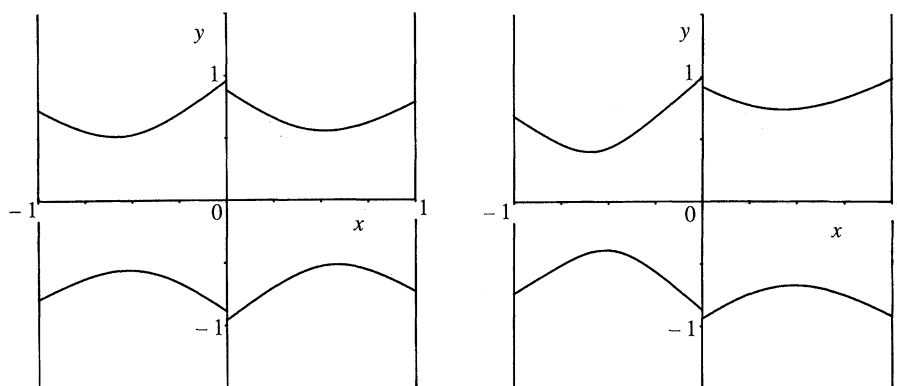


Figure 3 (left). Symmetric period-1 response at $\omega = 1$, $d = 1$, $r = q = 0.925$ for $\beta = 0.6$.

Figure 4 (right). Asymmetric period-1 response at $\omega = 1$, $d = 1$, $r = q = 0.925$ for $\beta = 0.7$.

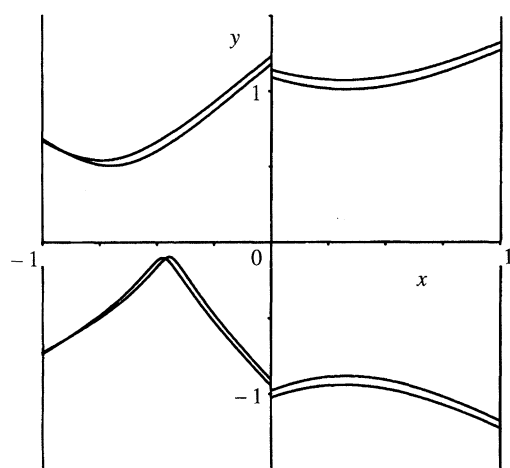


Figure 5. Asymmetric period-2 response at $\omega = 1$, $d = 1$, $r = q = 0.925$ for $\beta = 0.84$.

The agreement is excellent given that two distinct methods were used. The final orbit is shown in figure 3. It can be seen to be rotationally symmetric. The Poincaré point corresponding to the forcing at $t = 0 \pmod{2\pi}$ is at $(x, y) = (-0.9162, -0.7274)$.

The simplest way, numerically, to move around parameter space is to use this point as the starting conditions at $t = 0$ for a slightly different value of β and integrate until an asymptotically stable solution is found. Thus in figure 4 we find that at $\beta = 0.7$, the solution has undergone a symmetry-breaking bifurcation as one of the eigenvalues crosses the unit circle. One of the branches is exhibited here. Note the physical result that one wall is now being impacted on with a far higher velocity than the other and so there is a difference in energy transfer.

A further increase in β to 0.84, shows in figure 5 a period-2 solution with Poincaré points at $(-0.640, -0.344)$ and $(-0.588, -0.303)$, the result of a period-doubling bifurcation. Further period doublings may be expected, with the possibility of chaos being observed.

The choice of symmetrically placed walls has led to the first bifurcation in this sequence being a symmetry-breaking type. Asymmetrically placed walls will lead to asymptotic solutions whose first bifurcation will be period-doubling.

7. Conclusion and Discussion

The problem of a rigid block rocking between and impacting with two symmetrically placed side-walls has been considered. A method has been given which enables asymptotically stable periodic responses to be calculated for all values of the system parameters. An illustrative example has been given which shows both symmetry-breaking and period-doubling bifurcations.

Two main conclusions flow from this work. First, periodic responses are possible in this system. Second, the bifurcations lead to higher impact velocities on one side-wall than might be expected from pure extrapolation of the symmetric results. This in turn leads to higher energy transfer and may therefore have implications for the design of and wear on such structures.

Finally we note the intriguing possibility of these solutions co-existing in parameter space with solutions which oscillate between the walls, but do not touch them (as in Hogan 1989). Certainly the example given here corresponds to toppling solutions for $\beta = 0.6, 0.7$ and 0.84 in the absence of side-walls (figure 12 of Hogan 1989), these points lying far outside the stability areas of periodic responses. But the following scenario may be possible. The block oscillates freely between the side-walls for a given value of β (say) without impacting them. An increase in β to β_0 leads to the unique solution of impacting the side-walls with zero velocity, that is the horizontal extent of rocking is given by d . A further increase in β will lead to a bifurcation from non-impacting solutions to solutions which impact the side-walls. It may then happen that a decrease in β below β_0 produces a continuation of these solutions and hence have both types of solution co-existing. The resolution of this point lies in further study of this problem.

Appendix

The matrix N is given by

$$N = \frac{1}{\det \mathbf{D}} \begin{pmatrix} D_{22} & -D_{12} \\ rD_{21} & -rD_{11} \end{pmatrix}$$

where

$$\begin{aligned} \mathbf{D} &= \begin{pmatrix} D_{11} & D_{12} \\ D_{21} & D_{22} \end{pmatrix} \\ &= \begin{pmatrix} \mathcal{Q} & ch_{10} \\ \mathcal{S} & sh_{10} \end{pmatrix}^{-1} \begin{pmatrix} \mathcal{P} & 1 \\ \mathcal{R} & 0 \end{pmatrix} \begin{pmatrix} 1 & 0 \\ 0 & -1/q \end{pmatrix} \begin{pmatrix} \mathcal{U} & ch_{21} \\ \mathcal{W} & sh_{21} \end{pmatrix}^{-1} \begin{pmatrix} \mathcal{T} & 1 \\ \mathcal{V} & 0 \end{pmatrix} \end{aligned}$$

and $\mathcal{P}, \mathcal{Q}, \mathcal{R}, \mathcal{S}, \mathcal{T}, \mathcal{U}, \mathcal{V}$ and \mathcal{W} are all defined at the end of §4. N can be considered as the product of two matrices corresponding to impacts and two corresponding to free flight.

References

- Hogan, S. J. 1989 On the dynamics of rigid block motion under harmonic forcing. *Proc. R. Soc. Lond. A* **425**, 441–476.
- Hogan, S. J. 1990 The many steady state responses of a rigid block under harmonic forcing. *Int. J. Earthquake Eng. Struct. Dyn.* **19**, 1057–1071.
- Hogan, S. J. 1992a The effect of damping on rigid block motion under harmonic forcing. *Proc. R. Soc. Lond. A* **437**, 97–108.
- Hogan, S. J. 1992b On the motion of a rigid block, tethered at one corner, under harmonic forcing. *Proc. R. Soc. Lond. A* **439**, 35–46.
- Phil. Trans. R. Soc. Lond. A* (1994)

- Hogan, S. J. 1992*c* Heteroclinic bifurcations in damped rigid block motion. *Proc. R. Soc. Lond. A* **439**, 155–162.
- Housner, G. W. 1963 The behaviour of inverted pendulum structures during earthquakes. *Bull. seism. Soc. Am.* **53**, 403–417.
- Ishiyama, Y. 1982 Motions of rigid bodies and criteria for overturning by earthquake excitations. *Int. J. Earthquake Eng. Struct. Dyn.* **10**, 635–650.
- Kirkpatrick, P. 1927 Seismic measurements by the overthrow of columns. *Bull. seism. Soc. Am.* **17**, 95–109.
- Milne, J. 1881 Experiments in observational seismology. *Trans. seism. Soc. Japan* **3**, 12–64.
- Milne, J. 1885 Seismic experiments. *Trans. seism. Soc. Japan* **8**, 1–82.
- Milne, J. & Omori, F. 1893 On the overturning and fracturing of brick columns by horizontal applied motion. *Seismol. J. Japan* **17**, 59–86.
- Omori, F. 1899 Research on fracturing and overturning columns. (Report on seismic experiments by shaking table.) *Publ. Earthquake Invest. Committee* **28**, 4–69.
- Omori, F. 1900 On the overturning and sliding of columns. *Publ. Earthquake Invest. Committee* **32**, 19–33.
- Omote, S., Miyake, A. & Narahashi, H. 1977 Maximum ground acceleration in the epicentral area – Field studies on the occasion of the Ohita earthquake, Japan of April 21, 1975. *Bull. Int. Inst. seism. Earthquake Eng.* **15**, 67–82.
- Oppenheim, I. J. 1992 The masonry arch as a four-link mechanism under base motion. *Int. J. Earthquake Eng. Struct. Dyn.* **21**, 1005–1017.
- Perry, J. 1881 Note on the rocking of a column. *Trans. seism. Soc. Japan* **3**, 103–106.
- Psycharis, I. N. 1990 Dynamic behaviour of rocking two-block assemblies. *Int. J. Earthquake Eng. Struct. Dyn.* **19**, 555–575.
- Wong, C. M. & Tso, W. K. 1989 Steady state rocking response of rigid blocks. Part 2: Experiment. *Int. J. Earthquake Eng. Struct. Dyn.* **18**, 107–120.